International Conference on Mathematics, Computational Methods & Reactor Physics (M&C 2009)
Saratoga Springs, New York, May 3-7, 2009, on CD-ROM, American Nuclear Society, LaGrange Park, IL (2009)

A LINEAR SIMC SCHEME SUITABLE FOR EXTENSION TO MULTI-DIMENSIONS

Richard P. Smedley-Stevenson
AWE
Aldermaston, Reading, Berkshire, RG7 4PR, UK.
richard.smedley-stevenson@awe.co.uk

ABSTRACT

The aim of this paper is to present results from explorations into the viability of extending the slab geometry SIMC schemes developed by Brooks et al. for thermal radiation transport to multi-dimensions. Key to this extension is the ability to efficiently solve the resulting set of non-linear equations, which may require modifications to the finite element formulation in order to provide a robust numerical scheme.

Key Words: SIMC, linear discontinuous finite elements, asymptotic diffusion limit

1. INTRODUCTION

Slab geometry symbolic Implicit Monte Carlo (SIMC) schemes have been developed by Brooks et al. in slab geometry [1]. These schemes employ a linear finite element approximation for the spatial variation of either the equilibrium radiation energy density or the temperature field. Their studies indicated that the former approach was unsuitable for problems with steep wave-fronts. However, the latter scheme is unsuitable for extension to multi-dimensions due to the large number of different source terms (and associated symbolic unknowns) required to model the thermal emission process.

We have focused our efforts on developing schemes based on a linear treatment of both variables, which are consistent only at the nodes of the finite element approximation. This approach is commonly employed in deterministic simulations of thermal radiation transport problems, which are based on a linearized form of the material energy equation [2]. We compare this approach with that of Brooks et al. in order to highlight its shortcomings. However, despite the limitations, we believe this represents a viable scheme for efficiently solving multidimensional problems.

2. NUMERICAL SCHEMES

We begin by describing the equations of thermal radiation transport for a purely absorbing gray medium. The transport equation

$$\left[\frac{1}{c}\frac{\partial}{\partial t}+\underline{\Omega}\cdot\nabla+\sigma_a\right]I=\tfrac{1}{4\pi}\sigma_a B \tag{1}$$

corresponds to the propagation of photons along a unit direction vector Ω propagating at the speed of light c, subject to absorption with cross-section σ_a in units of 1/length. Photons are injected into the medium at the left hand boundary,

$$I(x=0,\Omega,t)=I_0, \qquad \Omega\cdot\hat{x}>0 \tag{2}$$

and also due to thermal emission from the heated material, assuming the material is in thermal equilibrium.

The corresponding material energy equation,

$$C_V\frac{\partial T}{\partial t}=c\sigma_a\left(\int_{4\pi} I\,d\Omega-B\right) \tag{3}$$

relates the net amount of energy radiated by medium to the change in the material energy, which is a assumed to vary linearly with temperature according to the heat capacity C_V, the material energy density per unit temperature. Here the blackbody radiation energy density B is related to the temperature by the radiation constant a, $B=aT^4$ and this corresponds to the equilibrium state for the radiation energy density $J=\int_{4\pi} I\,d\Omega$.

Brooks et al. [1] considered two different schemes, one where the blackbody equilibrium energy density is treated as a linear function and the other where the material temperature is treated as a linear function. We discount the former scheme as it is unable to handle the presence of steep wave-fronts. Instead we concentrate on the linear temperature scheme and reproduce the details of the method in the following section.

2.1. Consistent Linear Scheme

The material temperature T is discretized using finite element shape functions. In slab geometry we define two linear shape functions in each element, the left shape function $\chi_{i1}(x)$ is equal to unity at the left hand side of the cell and reduces to zero at the right hand end, likewise the right shape function $\chi_{i2}(x)$ is equal to zero at the left hand end and unity at the right hand end of cell i and both are defined to be zero outside of cell i. The material temperature can be expressed in terms of the values at the left and right hand end of the cell as,

$$T(x)=\sum_{j=1}^{2} T_{ij}\chi_{ij}(x), \qquad x_{i-1/2}<x<x_{i+1/2} \tag{4}$$

where $x_{i-1/2}$ and $x_{i+1/2}$ are the left and right hand boundaries of cell i. Note that the temperature is allowed to multi-valued at the interface between neighboring cells as we make make no assertions about continuity of the material temperature. The analysis by Clouët and Samba [3] indicates that the temperature field will tend towards continuity as the optical depth of the medium increases.

The blackbody equilibrium radiation field is derived directly from the expression for the temperature,

$$\begin{aligned} B(x) &= a\,T(x)^4 = a\left(T_{i1}\chi_{i1}(x)+T_{i2}\chi_{i2}(x)\right)^4 \\ &= a\left(T_{i1}^4\chi_{i1}(x)^4+4\,T_{i1}^3T_{i2}\chi_{i1}(x)^3\chi_{i2}(x)+6\,T_{i1}^2T_{i2}^2\chi_{i1}(x)^2\chi_{i2}(x)^2\right. \\ &\qquad \left.+4\,T_{i1}T_{i2}^3\chi_{i1}(x)\chi_{i2}(x)^3+T_{i2}^4\chi_{i2}(x)^4\right) \\ &= a\left(T_{i1}^4\chi_{i1}(x)^4+4\,T_{i:3,1}^4\chi_{i1}(x)^3\chi_{i2}(x)+6\,T_{i:2,2}^4\chi_{i1}(x)^2\chi_{i2}(x)^2\right. \\ &\qquad \left.+4\,T_{i:1,3}^4\chi_{i1}(x)\chi_{i2}(x)^3+T_{i2}^4\chi_{i2}(x)^4\right) \end{aligned} \tag{5}$$

In order to model the emission term using symbolic particles we require each term in this expression to be allocated its own symbolic unknown so that the final particle weight can be expressed as a linear combination of these unknowns. This means that the energy deposition matrix is now of size $2N$ by $5N$, where N is the number of cells in the problem, which makes it significantly more expensive to invert than the N by N matrix associated with the piecewise constant scheme.

Brooks et al. postulate a sampling scheme based on the difference formulation (where an offset function is subtracted from the radiation intensity), but it is easy to extend their sampling strategies to this scheme, which is an intensity based version of their SIMC formulation. We have various choices for sampling the thermal emission particles, which affect the amount of statistical noise in the results, however the details of the sampling scheme do not alter the broad conclusions in terms of the robustness of the resulting computational method provided that we retain the leading order cancellation between the emission and absorption terms in opaque media.

Specifically, the emission and absorption tallies should cancel each other on a per particle basis i.e. in a point-wise sense, rather than relying on averaging over the ensemble in order to achieve a cell-wise energy balance. Erroneous results were obtained from an early implementation where the statistical noise was removed from the emission term only, leading to incorrect wave shapes and a failure to correctly propagate the radiation front.

The Galerkin weighted material energy equation is given by,

$$\begin{aligned} \left\langle \int C_V \frac{\partial T}{\partial t}(x)\chi_{ij'}(x) \right\rangle &= \sum_{j=1}^{2} \int C_V \chi_{ij}(x)\chi_{ij'}(x)\,dx \frac{\partial T_{ij}}{\partial t} \\ &= \int c\sigma_a \left(\int_{4\pi} I\,d\Omega - B \right) \chi_{ij'}(x)\,dx \\ &= \langle c\sigma_a J \chi_{ij'} \rangle - \langle c\sigma_a B \chi_{ij'} \rangle \end{aligned} \tag{6}$$

and this is supplemented by additional equations for the extra symbolic unknowns,

$$T_{i:3,1}^4 = T_{i1}^3 T_{i2}, \quad T_{i:2,2}^4 = T_{i1}^2 T_{i2}^{2,} \quad T_{i:1,3}^4 = T_{i1} T_{i2}^3 \tag{7}$$

so that the resulting set of 5 equations per cell can be solved using a globally convergent version of Newton's method.

For linear triangular elements the consistent expression for the blackbody function yields 15 separate terms and 12 additional symbolic unknowns, in the expression for the fourth power of the temperature. This increases to 35 terms for quadrilateral and/or tetrahedral elements, while a hexahedral element will have a total of 330 individual terms. Consequently, the number of terms required to model the thermal emission term makes extending this scheme into multi-dimensions impractical despite its desirable properties.

2.2. Multiple Linear Scheme

In the multiple linear scheme proposed in this paper, we replace the representation of the blackbody function as a quartic function which is fully consistent with the temperature variation with the following approximate form,

$$B(x) = a\,T(x)^4 = a\left(T_{i1}^4 \chi_{i1}(x) + T_{i2}^4 \chi_{i2}(x)\right) \tag{8}$$

which agrees with the consistent representation at the nodes of the element but varies linearly within each element. This term can be modeled by using the values of T^4 at either end of the cell as the symbolic unknowns and consequently no additional unknowns are required to supplement the Galerkin weighted energy equation.

2.3. Solving the SIMC Energy Equation

The SIMC energy equation is discretized in time using backward Euler time differencing in order to arrive at the fully implicit version of the SIMC method. Monte Carlo particles are sourced according to the thermal emission source term in the right hand side transport equation, with symbolic weights which are linear combinations of the T^4 unknowns. During the tracking step the energy deposition is recorded in terms of these symbolic unknowns in a sparse matrix structure and this set of non-linear equations is inverted in order to determine the values of the symbolic unknowns at the end of the current time-step.

This information is then used to update the particle weights for those which reached census; these particles will have a fixed (known) weight on subsequent time-steps. We use this information to update the energy deposition tallies so they are consistent with the updated particle weights. This allows us to solve an energy equation for the symbolic unknowns which differs from that corresponds to the enforcement of energy balance for the current time-step.

This allows us to make various additional approximations when formulating the SIMC energy equation, such as ignoring variations in the heat capacity of the material during the time-step, without impacting on the accuracy of the energy balance achieved during the time-step. This enables us to take into account non-linear variations in the material energy, by calculating new material temperature values which are consistent with the material energies from the equation of state (EOS) tables after the solution of the SIMC equations. This is preferable to allowing thermodynamic inconsistencies in the EOS tables to upset the convergence of the SIMC energy equation.

2.4. Comparison of the Different Approximations

The integrals of the shape functions can be performed in closed form,

$$\begin{gathered}\langle \chi_{i1}^2 \rangle = dx_i/3, \ \langle \chi_{i1}\chi_{i2} \rangle = dx_i/6, \\ \langle \chi_{i1}^5 \rangle = dx_i/6, \ \langle \chi_{i1}^4\chi_{i2} \rangle = dx_i/30, \ \langle \chi_{i1}^3\chi_{i2}^2 \rangle = dx_i/60\end{gathered} \tag{9}$$

and the other values follow from symmetry considerations; the brackets indicate averaging over the problem domain. We can use this to work out the time evolution behavior for this element in the different schemes. Inverting the mass matrix (which is only possible by virtue of using a discontinuous representation of the material temperature), the material energy equation can be written as

$$C_V \begin{bmatrix} \partial T_{i1}/\partial t \\ \partial T_{i2}/\partial t \end{bmatrix} = \frac{2}{dx_i} \begin{bmatrix} 2 & -1 \\ -1 & 2 \end{bmatrix} \begin{bmatrix} \langle c\sigma_a J \chi_{i1} \rangle - \langle c\sigma_a B \chi_{i1} \rangle \\ \langle c\sigma_a J \chi_{i2} \rangle - \langle c\sigma_a B \chi_{i2} \rangle \end{bmatrix} \tag{10}$$

We can now insert the corresponding expressions for the blackbody energy density in the right hand side of the energy equation, to obtain expressions which apply in the absence of statistical noise from the discrete sampling of the emission source. For the consistent linear scheme we obtain,

$$C_V \begin{bmatrix} \partial T_{i1}/\partial t \\ \partial T_{i2}/\partial t \end{bmatrix} = \frac{2}{dx_i} \begin{bmatrix} 2 & -1 \\ -1 & 2 \end{bmatrix} \begin{bmatrix} \langle c\sigma_a J \chi_{i1} \rangle \\ \langle c\sigma_a J \chi_{i2} \rangle \end{bmatrix} - \frac{1}{5} \begin{bmatrix} 3 & 2 & 1 & 0 & -1 \\ -1 & 0 & 1 & 2 & 3 \end{bmatrix} c\sigma_a \begin{bmatrix} B_{i1} \\ B_{i1}^{3/4} B_{i2}^{1/4} \\ B_{i1}^{1/2} B_{i2}^{1/2} \\ B_{i1}^{1/4} B_{i2}^{3/4} \\ B_{i2} \end{bmatrix} \tag{11}$$

which means that for $B_{ir} = 0$ the right node is being heated by the thermal emission from the element (rather than being cooled), which explains the greater robustness observed for this scheme. For the multiple linear approximation we have

$$C_V \begin{bmatrix} \partial T_{i1}/\partial t \\ \partial T_{i2}/\partial t \end{bmatrix} = \frac{2}{dx_i} \begin{bmatrix} 2 & -1 \\ -1 & 2 \end{bmatrix} \begin{bmatrix} \langle c\sigma_a J \chi_{i1} \rangle \\ \langle c\sigma_a J \chi_{i2} \rangle \end{bmatrix} - c\sigma_a \begin{bmatrix} B_{i1} \\ B_{i2} \end{bmatrix} \tag{12}$$

and the emission process removes energy in direct proportion to the corresponding nodal value of the blackbody energy density. For one sided heating, the heated node cools 1.67 times as fast compared with the corresponding node in the consistent scheme, but leaves the energy of the cold node unaltered, which means that overall the cell is cooling 2.5 times faster.

Obviously, the differences between the two schemes get smaller as the nodal values of the blackbody function in the element get closer together. Expanding the blackbody function in a Taylor series about the mean value in the element we have,

$$C_V \begin{bmatrix} \partial T_{i1}/\partial t \\ \partial T_{i2}/\partial t \end{bmatrix} \approx \frac{2}{dx_i} \begin{bmatrix} 2 & -1 \\ -1 & 2 \end{bmatrix} \begin{bmatrix} \langle c\sigma_a J \chi_{i1} \rangle \\ \langle c\sigma_a J \chi_{i2} \rangle \end{bmatrix} - c\sigma_a \begin{bmatrix} B_{i1} \\ B_{i2} \end{bmatrix} + \frac{1}{16} c\sigma_a \frac{(B_{i2} - B_{i1})^2}{\frac{1}{2}(B_{i1} + B_{i2})} \tag{13}$$

for the consistent formulation which is accurate to second order in the difference between the nodal values. It is the last term on the right hand side which illustrates the onset of the difference between the two formulations as the nodal values start to diverge.

One problem we do have with the algorithm is the possibility of generating negative solutions due variations in the energy absorbed across the cell. There is the potential for the absorption term to produce negative values for the nodal temperatures once the ratio of the scored values exceeds a factor two. The multiple linear scheme is more likely to be subject to this error due to the larger emission rate associated with this scheme and the fact that the cold end of the cell stays cold rather than being heated by the thermal emission from the hot side.

This problem is exacerbated by the presence of the statistical noise from the Monte Carlo solution of the transport equation. If we assume that the absorption tallies corresponding to the left and right shape functions have the same normal distribution corresponding to a uniform intensity field in the cell, then we see an increase in the variance of the point-wise energy absorption by a factor $\sqrt{5}$ relative to the tallies associated with the multiplication by the inverse of the mass matrix; these tallies are themselves potentially a factor $\sqrt{2}$ more noisy than the cell absorption tally. This explains why the piecewise linear scheme produces temperature values which are potentially > 3 times more noisy than the original piecewise constant formulation. This will have an even greater impact on multi-dimensional simulations.

3. COMPUTATIONAL STRATEGY

3.1. Attempting to Solve the Full Non-linear System

In order to guarantee that we can solve the non-linear energy equation associated with the SIMC method we need to ensure that the resulting equations have a physical i.e. positive temperature solution. Unfortunately, we cannot determine this a priori. Our current preferred strategy is to modify the definition of the temperature as a function of T^4 below a user specified cut-off temperature value, to ensure that it remains well behaved in circumstances where $T^4 < 0$. Various different approximations have been tried for extending the definition of the temperature, with the most successful being a quadratic which matches the first and second derivatives at the cut-off temperature.

We use the non-linear solvers from the PETSc toolkit [4] to solve the resulting non-linear equations. If we are able to obtain a converged solution to the non-linear system, we then artificially reduce the slope in any cell which produces a negative T^4 value to ensure we . In circumstances where the solver fails to converge to a solution of the system of equations, we can revert to solving the linearized material energy equation.

The need to solve a system of non-linear equations can be circumvented completely by linearized energy equation according to the procedure described in the next section. However, the lack of

consistency introduced by this approximation will destroy the unconditional stability of the SIMC method. Consequently, it is recommended than an attempt be made to solve the full non-linear system, despite the additional overheads associated with solving a non-linear system of equations.

3.2. Linearization of the Energy Equation

So far we have been considering obtaining a consistent solution of the fully non-linear form of the energy equation. An alternative strategy is to linearize the time-derivative term i.e.

$$C_V \frac{\partial T}{\partial t} \approx \frac{C_V}{4 a T^3} \frac{\partial B}{\partial t} = \beta^{-1} \frac{\partial B}{\partial t} \tag{14}$$

so that the revised energy equation can be written as,

$$\left\langle \left(\beta^n\right)^{-1} \Delta t \frac{\partial B}{\partial t}(x) \chi_{ij'}(x) \right\rangle = \int c \Delta t \sigma_a \left(\int_{4\pi} I \, d\Omega - B \right) \chi_{ij'}(x) \, dx \tag{15}$$

where the superscript indicates that β is evaluated using the start of time-step temperatures.

Linearization can be employed with the consistent linear scheme, however in this case there are still non-linear terms in the formulation associated with the modeling of the thermal emission sources which may still lead to a lack of robustness when attempting to solve the material energy equation. For the multiple linear approximation scheme, the material energy equation is now a linear function of the blackbody energy density unknowns.
We note that the β coefficient can be modeled as either a cell centered or discontinuous node centered quantity, the latter being more accurate and better able to prevent excess energy flowing through cold cells. The converged non-linear solution is equivalent to defining

$$\beta^{-1} = C_V \Delta T / \Delta B \tag{16}$$

and converging the values of the change in the temperature ΔT and blackbody energy density ΔB during the current time-step.

The benefit of this approach is that we can always obtain a solution for the resulting set of linear equations, even if it is non-physical, provided that the coefficient matrix is non-singular; this can be guaranteed by choosing a small enough time-step so that the time-derivative term dominates the equations. As a consequence, we can be more cautious in applying robustness modifications (such as mass lumping), as they are no longer required simply to enable us to solve the resulting equations. Furthermore, rather than modifying the finite element formulation, we can instead apply simple fix-ups to the solution in order to prevent any non-physical behavior; by default we employ the post processing step described in the previous section on solving the non-linear equations.

The downside of linearization is that it allows departures from equilibrium to develop when either we fail to resolve transient behavior and/or the solution is contaminated by statistical

noise, features inherited from the IMC method. We can illustrate this issue by considering the behavior in an infinite medium. For simplicity we assume that the background radiation energy density stays constant (which eliminates the source of noise in the simulation) and consider the equilibration of the material due to heating from this background field. A fully implicit (backward Euler) temporal discretization leads to the following expression for the temperature at the end of the current time-step,

$$C_V T^{n+1} + \sigma_a c \Delta t B^{n+1} = C_V T^n + \sigma_a c \Delta t J \tag{17}$$

where J is the radiation energy density. The equivalent expression corresponding to the linearized energy equation is,

$$\left(1 + \beta^n \sigma_a c \Delta t\right) B = B^n + \beta^n \sigma_a c \Delta t J \tag{18}$$

and this replaces the thermal emission term in the previous expression to yield an expression for the linearized temperature,

$$C_V T^{n+1} = C_V T^n + \frac{\sigma_a c \Delta t}{1 + \beta^n \sigma_a c \Delta t} (J - B^n) \tag{19}$$

which we recognize as the material energy equation from the IMC method. This equation can overshoot the equilibrium temperature value at the end of the first time-step if $\beta^n \sigma_a c \Delta t \geq 4 (B^n / J)^{3/4}$ i.e. $\sigma_a c \Delta t \geq (B^n J^3)^{-1/4} C_V T^n$ assuming that $J \gg B^n$. This occurs because we are effectively ignoring the re-emission process during the first time-step when we linearize this equation.

We illustrate this behavior for a problem with $\sigma_a = 200\,\mathrm{cm}^{-1}$, $C_V = 10^8\,\mathrm{J/cm^3/keV}$ where the material temperature is initially at 0.01 keV and the radiation field is kept at a temperature of 1keV. The material temperature evolution is then tracked for different values of the time-step, with the results displayed in Fig. 1. This problem was motivated by studying the temperature evolution of the point closest to the blackbody radiation drive in the Marshak wave problem we consider in the results section. The slope of the heating rate for the linearized equations is essentially constant due to the small initial value of β^n. Consequently, for the linearization scheme we must choose an initial time-step which is small enough so that we do not overheat the material. This time-step limit is not always easy to determine a priori, but we note that Wollaber [5] has made significant progress in this area for the IMC method.

For smaller values of the time-step the linearized solution turns out to be more accurate, but we can see that the fully implicit solution associated with the converged non-linear scheme has the benefit that it never overheats the material irrespective of how large we set the initial time-step. Furthermore, for large time-steps the fully implicit method guarantees that the problem comes into equilibrium after a single time-step, which is important for simulations where the statistical noise may be sufficient to artificially drive the solution out of equilibrium.

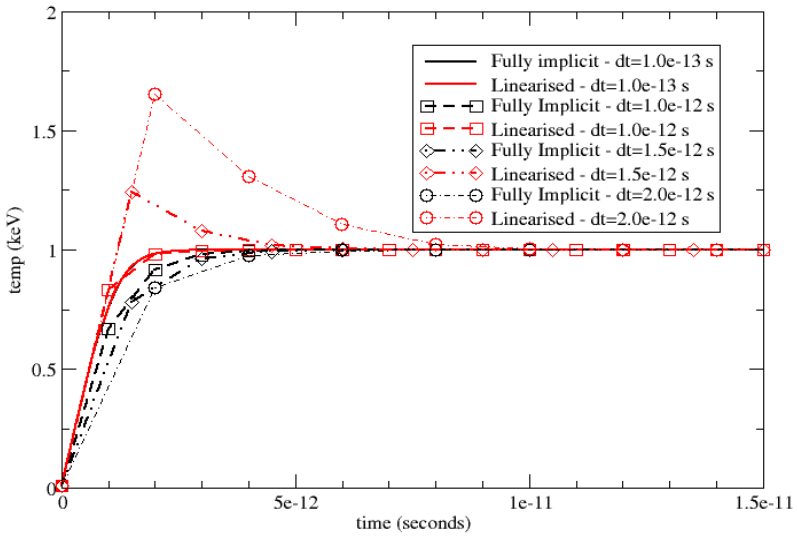

Fig. 1. Study of the effect of linearization on the heating rate in an infinite medium. For large time-steps the temperature obtained from solving the linearized equations overshoots the equilibrium value and the material then has to cool into equilibrium. The fully implicit solution never overshoots, but does tend to overestimate the amount of thermal emission and is therefore less accurate than the linearization scheme for small enough time-steps.

3.3. Time-step Selection

As we attempt to temporally converge the results of a simulation (either by employing a time-stepping algorithm which controls the change in the temperature during the time-step, or by fixing the time-step according to the known characteristics of the problem being modeled), either technique for modeling the temporal evolution becomes an equally valid approach for solving the transport problem. Furthermore, we are still neglecting the temperature dependence of the material properties when solving the non-linear energy equation, so it could be argued that the error which arises from not updating the opacity may dominate that associated with linearizing the time-derivative term in more realistic applications.

The best way to address the issue of whether we can reliably solve the SIMC energy equation is to enforce some form of time-step control (based on the cell averaged temperature change during the time-step). This allows us to ensure that when attempting to solve the full non-linear equations we have a starting guess which is sufficiently close to the converged solution. This will give the non-linear solvers a fighting chance to be able to converge the solution of the SIMC equation, even if the temperature solution contains some undershoots in regions where there are steep gradients. Furthermore, it ensures that the solution of the linearized equations remains a reasonable approximation of the full non-linear equations, whichever set of equations we choose to solve for the symbolic particle weights.

4. RESULTS

In this section we compare the performance of the new scheme with the consistent linear finite element scheme for the material temperature proposed in reference 1. Specifically, we investigate the steady-state convergence for the flow of radiation through a five mean free path thick slab with a 1 keV blackbody source applied at the left hand end; the thermal heat capacity of the slab is 10^8 J/cm^3/keV. Brooks et al. used this problem to illustrate the superior spatial convergence of the method based on a consistent linear representation of the blackbody energy density, compared with the consistent linear treatment of material temperature, for cells one mean free path thick.

In Fig. 2 we illustrate the spatial convergence of the results as the problem reaches steady-state. The new scheme is slightly less accurate than the consistent linear scheme, but still produces reasonable results on this coarse mesh. Fig. 3 illustrates the time-dependent behavior, where we observe that the solution undershoots in the cell next to the drive. This problem uses an initial non-zero temperature in order to enable physical solutions to be obtained despite the presence of this undershoot and we compare various mass lumping options which can be employed in order to obtain a robust solution. Note that the opacity of the slab has been increased so that it is now 10 mean free paths thick, to match the results from reference [1].

In the "double lumping" strategy both the time derivative term and the thermal emission term are "mass lumped" i.e. the corresponding matrices are replaced by a diagonal matrix formed from their row sums, so that the energy associated with each node can be directly related to the symbolic unknown at that node, rather than as a linear combination of the values at all the nodes. These results illustrate the dramatic reduction in point-wise accuracy which occurs when we mass lump the different terms in the SIMC energy equation.

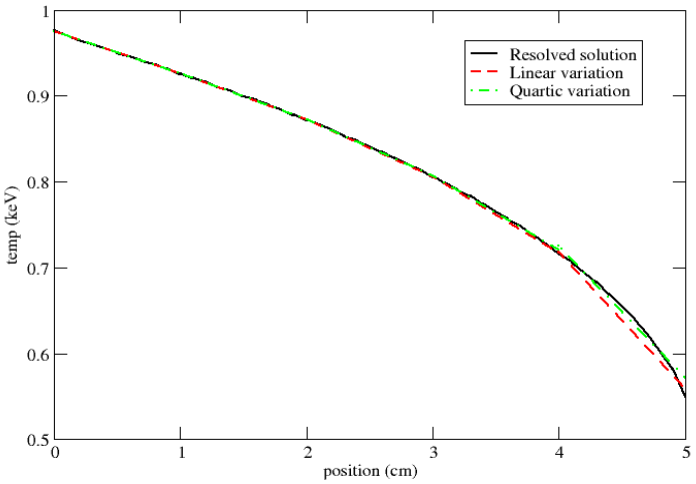

Fig. 2. Comparison of the steady-state solutions for radiation flow through a 5 mean free path thick slab. Here we compare a converged 50 zone solution with 5-zone solutions obtained for the multiple linear scheme (temperature and blackbody energy density both linear) and the consistent linear scheme.

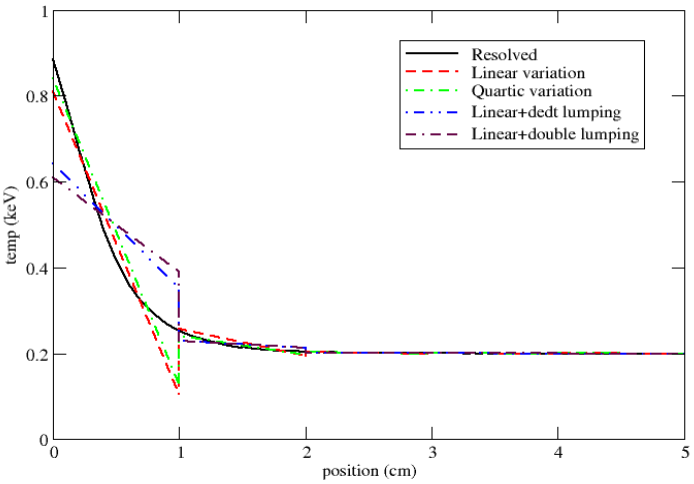

Fig. 3. Comparison of the different lumping schemes applied to a time dependent problem. Here the slab is 10 mean free paths thick and starts in thermal equilibrium at 0.2 keV, heated by a 1 keV blackbody source at the left hand end. These results were generated with a time-step of 10^{-11} seconds and the results are plotted at a time of 3.5×10^{-10} seconds after the drive is applied.

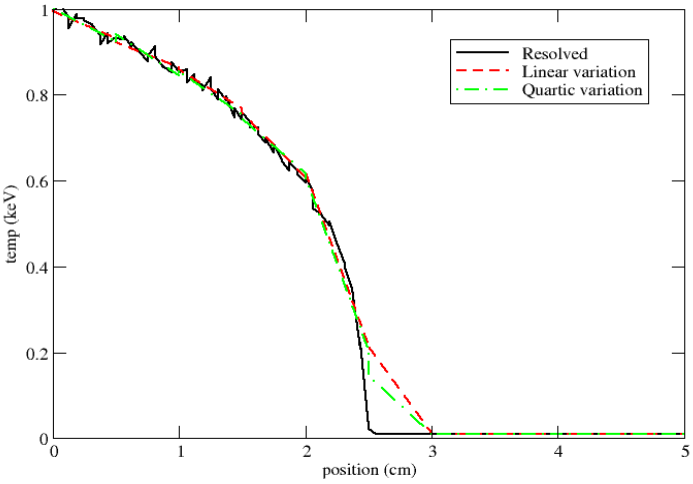

Fig. 4. Comparison of the scheme for the Marshak wave problem at 3×10^{-7} seconds after the drive is applied. Here we compare the solutions obtained with 10 cells (100 mean free paths per cell) with the converged 80 cell (12.5 mean free paths per cell) solution.

Finally, in Fig. 4 we present results for a Marshak wave propagation problem discussed in section 3.2. This is the key motivator for this work, as although optically thin systems can be accurately modeled by using the piecewise constant formulation, a piecewise linear scheme is essential in order to correctly predict the propagation velocity for a radiation wave traveling through an unresolved opaque medium. Again we see that the results from the scheme proposed in this paper are comparable in terms of accuracy with the consistent linear scheme of Brooks et al. [1].

5. CONCLUSIONS

In this paper we have presented an alternative to the linear SIMC scheme of Brooks et al. [1]. Our scheme has the advantage of being easier to implement in multi-dimensions, whilst also providing similar accuracy to the original scheme. We have explored the difficult issue of obtaining robust solutions of the resulting non-linear SIMC material energy equation, a task which was made significantly easier by restricting the implementation to solving slab geometry problems. This analysis has allowed broader conclusions to be developed about the application of these schemes to solving challenging multi-dimensional problems.

ACKNOWLEDGEMENTS

The author would like to acknowledge the hospitality of Eugene Brooks and his co-workers during a visit to LLNL in April 2007 and a follow-up discussion with Abe Szöke (kindly hosted by Dr Ardan Patwardhan in the Biochemistry department at Imperial College) which took place while Abe was visiting the UK in May 2007.

REFERENCES

1. E. D. Brooks III, A. Szöke, and J. D. L. Peterson, “Piecewise linear discretization of Symbolic Implicit Monte Carlo radiation transport in the difference formulation,” *Journal of Computational Physics*, **220**, pp.471-497 (2006).
2. J. E. Morel, B. T. Adams, T. Noh, J. M. McGhee, T. M. Evans, T. J. Urbatsch, “Spatial discretizations for self-adjoint forms of the radiative transfer equations,” *Journal of Computational Physics*, **214**, pp.12-40 (2006).
3. J.-F. Clouët, and G. Samba, “Asymptotic diffusion limit of the symbolic Monte-Carlo method for the transport equation”, *Journal of Computational Physics*, **195**, pp.293-319 (2004).
4. S. Balay, W. D. Gropp, L. C. McInnes, and B. F. Smith, “PETSc Users Manual”, ANL-95/11 - Revision 2.3.3, Argonne National Laboratory (2008).
5. A. B. Wollaber, “Advanced Monte Carlo Methods for Thermal Radiation Transport”, PhD dissertation, Nuclear engineering and Radiological Sciences and Scientific Computing Department, University of Michigan (2008).